J Mater Sci: Mater Electron (2023) 34:1221

The effect of fabrication method on physical properties of different Y211 and 20% Ag_2O added YBCO sample

Şeyda Duman[1,2,*], Bakiye Çakır[2], Mehmet Başoğlu[3], Tayfur Küçükömeroğlu[1], and Alev Aydıner[1]

[1] *Department of Physics, Faculty of Sciences, Karadeniz Technical University, 61080 Trabzon, Turkey*
[2] *Department of Medical Services and Techniques, Vocational School of Health Services, Artvin Çoruh University, 08000 Artvin, Turkey*
[3] *Department of Electric and Energy, Gümüşhane Vocational School, Gümüşhane University, 29100 Gümüşhane, Turkey*

Received: 17 March 2023
Accepted: 18 May 2023
Published online: 26 May 2023

ABSTRACT

In this study, it is aimed to investigate the effects of production methods on the physical properties of 20% Ag_2O and different ratios of Y211 added YBCO samples. In this context, the samples with Y123 + x % (x = 20, 25, 30) Y211 + 20%Ag_2O compositions were fabricated by MPMG and TSMG methods in two groups to join YBCO main samples. XRD measurements were performed to determine the characteristic peaks. Trapped magnetic fields and vertical levitation forces between the bulk samples and a permanent magnet were measured using a computer-controlled system in ZFC at 77 K. From the XRD measurements, it was found that MPMG YBCO samples had a dominant superconducting structure and partially showed orientation peaks in the c-axis direction, while TSMG YBCO samples were single-crystal samples oriented along the c-axis. From the trapped magnetic field measurement results, the trapped magnetic field value of the Y123 + 25%Y211 + 20%Ag_2O (TAg25) sample prepared by the TSMG method was higher than that of the other samples. Among the levitation force measurement results, the maximum repulsive force values of TAg25 and TAg30 (Y123 + 30%Y211 + 20%Ag_2O) samples are the highest. At the same time, the hysteresis widths of these samples are also the highest, which proves that their flux-pinning potential is higher than that of the other samples.

1 Introduction

Bulk $YBa_2Cu_3O_{7-x}$ (YBCO), one of the high temperature superconductors (HTS), has significant potential in engineering applications due to its transformation to superconductor at liquid nitrogen temperature [1] and its relatively higher current carrying capacity compared to other superconductors. To increase this potential in engineering applications, it is necessary to remove the grain boundaries present

Address correspondence to E-mail: seydaduman@artvin.edu.tr

https://doi.org/10.1007/s10854-023-10674-6

in the microstructure of superconducting materials. As these grain boundaries hinder the current carrying capacity.

The top seeded melt growth (TSMG) method, which is one of the melting methods, is a successful method in producing large and single-grain superconductor samples [2] but it is a limited method for producing much larger samples [3].

Unlike conventional permanent magnets, single-grain bulk superconductors scale with sample volume. This means that the larger the single-grain, the higher the current carrying capacity. Thus, the material can trap the larger magnetic field [2, 4, 5]. Therefore, the use of large single-grain samples is important in applications. Large superconducting samples need to be fabricated for use in various applications. Since bulk superconductors are fragile and it is difficult to produce very large samples with current methods, it is necessary to increase the size of the produced samples with suitable joining methods. In addition, the large-sized HTS materials are technologically important and can be used in a wide range of engineering applications, including nuclear magnetic resonance (NMR), trapped field magnets, flywheel energy storage, magnetic separation, and compact motors and generators [6–8]. However, when superconductors are joined, it is important that the current flow is not interrupted in the welding region. Therefore, a welding method using solder material has been developed.

The welding joint method is a joining method by placing a solder material with a relatively low melting temperature between the polished surfaces of two single-crystal bulk superconductors. The quality of the welding process using the solder material depends on the relationship between the YBCO single crystals and the BaCuO liquid phase. This melt makes it possible to combine the YBCO sample with the source material at a temperature below the peritectic temperature.

Adding Ag to the solder material lowers the melting temperature up to 40 °C compared to pure YBCO superconductors. The Ag-added YBCO superconductor is quite compatible with the crystal structure of the YBCO matrix. Ag particles fills the intergranular gaps by reducing the weak coupling effects that may occur in the welding region. At the same time, the distribution of Ag particles in the structure of Ag-added YBCO superconductors reduces the formation of micro-cracks in the *c*-axis direction and provides mechanical durability. In addition, non-superconducting structures such as Y_2BaCuO_5 (Y211) particles, CuO and Ba-rich phases are the factors that adversely affect the quality of the welding region.

The presence of secondary phases acts as a barrier for supercurrents and adversely affects welding region quality. Ag additive increases conductivity between superconducting bulks which welded and allows supercurrents to flow more easily. So it significantly increases the critical current density (J_c) [9–15]. At the same time, samples welded with Ag-added solder material exhibit a trapped magnetic field behavior comparable to single-grain samples. For these reasons, Ag-added YBCO superconductor is a good choice as a solder material [7, 8, 16–19].

Significantly, it is known that both the distribution and size of Y211 particles play an important role in the control and improvement of the superconducting properties of YBCO single grains [20]. If the dimension of Y211 particles is reduced in the welding region where residual phases can accumulate, there are no boundary gaps at the interface and the J_c value in the welding region is not interrupted [21].

The welding method allows to enlarge of sample sizes. In a previous study, a successful welding process with improved electrical and mechanical properties without disturbing the superconducting properties of the main matrix was made using the 17% Ag-added YBCO solder material produced by melt powder melt growth (MPMG) method [22]. The quality of the welding region depends on the quality of the solder material and connectivity between the solder material and main materials. The better the quality of the solder material, the better the performance of the welded bulk will be. It is important to determine suitable addition type, addition ratios and production methods to improve the properties of superconducting samples. In this study, with the aim of determining the most suitable method and composition in production of the solder material, superconducting samples were fabricated using both MPMG and TSMG methods in Y123 + x % Y211 ($x = 20$, 25 and 30) + 20%Ag_2O composition. The structural and physical properties of the superconducting samples were examined.

2 Experimental details

In order to obtain Y123 and Y211 powders, Y_2O_3, $BaCO_3$ and CuO starting powders were mixed in appropriate ratios and calcined at 900 °C for 36 h. The calcined Y123 powder was held at 1450 °C for 5 min and the molten material was poured onto a cupper plate at this temperature. It was, then, sandwiched with another cupper plate to protect phase condition during melting. The resulting plates were ground to powder again. While the ratio of Ag_2O additive in Y123 material is between 15 and 20%, the mechanical and electrical properties of the material are improved [23]. For this reason, Y123, Y211 and Ag_2O powders were mixed in appropriate ratios to produce superconducting samples in Y123 + x% (x = 20, 25, 30) Y211 + 20%Ag_2O composition to be used as solder material. Pellets with a diameter of 20 mm were pressed under 10 tons of pressure. The pellets were prepared in two groups. A group of the pellets was heated at 1030 °C and kept at this temperature for 1 h. Then it was rapidly cooled to 995 °C and slowly cooled between 995–935 °C for 100 h. So, MPMG samples were produced by the crystal growth process shown in Fig. 1. The second group of the samples was produced by TSMG method using a Nd123 seed for the growth of the samples in the c-axis direction. The crystal growth process in TSMG method was performed for 200 h unlike the MPMG method (Fig. 1). All samples prepared using MPMG and TSMG methods were annealed with oxygen for 200 h at 500 °C to show superconductivity properties. The samples produced in two groups are labeled as in Table 1. X-ray diffraction (XRD) patterns were obtained using CuKα (λ = 1.54059 Å, 40 kV, 30 mA) radiation with Rigaku D/Max III powder diffractometer to examine the crystal structures of the samples. The Surface microstructures were examined at 20× magnification using a Nikon Eclipse ME600 polarized light optical microscope to obtain information about crystal grain size, grain shape and distribution, cracks or other defects.

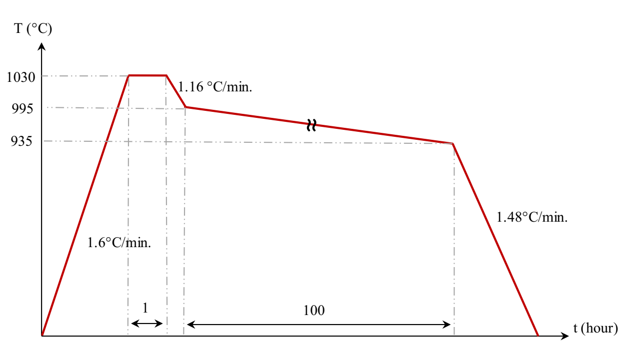

Fig. 1 The crystal growth schedule of the Y123 + x% (x = 20, 25, 30) Y211 + %20Ag_2O samples produced by MPMG method

In order to measure trapped magnetic fields in bulk superconductors, trapped magnetic field measurements were performed in a custom-built computer-controlled system, detailed information of which is given in reference [24], using a commercially purchased Nd magnet with 20 mm diameter and height and a maximum field value of ~0.5 T, at liquid nitrogen temperature (77 K). The vertical magnetic levitation forces between the bulk samples and the cylindrical NdFeB permanent magnet were measured under the ZFC regime with the same apparatus at 77 K.

3 Results and discussion

The X-ray diffraction patterns of MAg20, MAg25 and MAg30 samples produced by MPMG method are shown in Fig. 2, respectively. It is seen that all samples have characteristic superconducting peaks [indexed as (013) and (103)], as well as the presence of other superconductivity peaks and Y211 peaks defined as ref [25–27]. In addition, the presence of orientation peaks was observed in the samples (00ℓ) [28]. This indicates that although the sample has a granular structure, some of the existing grains are oriented in the c-axis. At the same time, it can be seen that the number of Y211 peaks of these samples is higher and the peak intensities are dominant.

The Ag_2O compound gives a characteristic peak of 100% at an angle of 32.8° [29]. The characteristic (103) superconducting peak of the Y123 compound is also seen at close angles to Ag_2O. When the X-ray diffraction patterns of the samples used in this study are examined, it is seen that the characteristic peak of the Ag_2O compound is embedded in the characteristic (103) superconducting peak. In addition, the presence of the Ag_2O peak at different angle values is clearly seen in all samples using the MPMG method.

The X-ray diffraction patterns of TAg20, TAg25 and TAg30 samples produced by the TSMG method are shown in Fig. 3, respectively. All samples have (00ℓ) peaks oriented in the c-axis direction.

Table 1 The names of the samples produced with MPMG and TSMG methods

Composition	MPMG sample name	TSMG sample name
Y123 + %20Y211 + %20Ag_2O	MAg20	TAg20
Y123 + %25Y211 + %20Ag_2O	MAg25	TAg25
Y123 + %30Y211 + %20Ag_2O	MAg30	TAg30

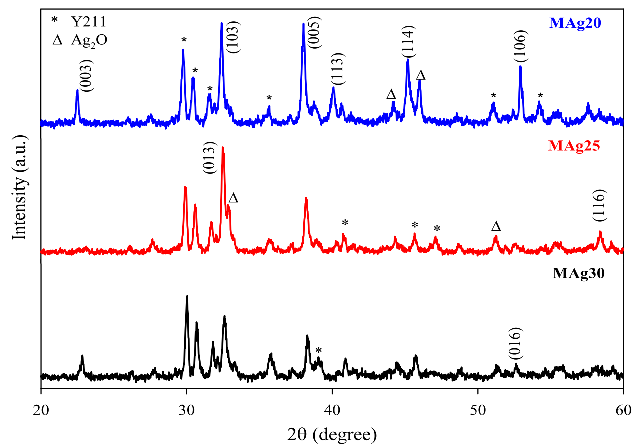

Fig. 2 XRD patterns of MPMG samples

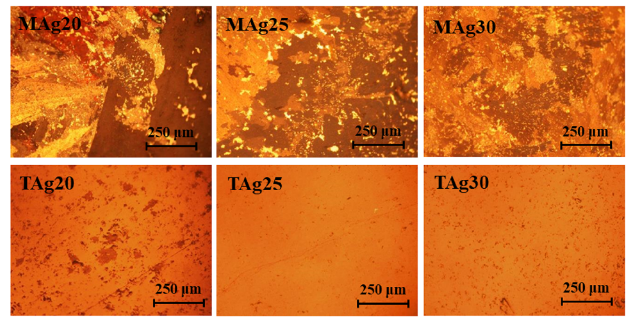

Fig. 4 Polarized optical photographs

Accordingly, it can be said that the TSMG samples are single crystals with preferential orientation. In addition, since the intensity of the (00ℓ) peaks is high, it suppressed the Ag_2O peaks. Therefore, Ag_2O peaks are not clearly visible in this figure.

Figure 4 shows polarized optical photographs of all samples taken at 20× magnification. From these photographs it can be seen that the Ag_2O added MPMG samples have a multi-grained structure. Different colour distributions represent grains with different orientations. The white bright areas seen on the surface of the samples are considered to be Ag_2O particles that are well dispersed in the sample [30]. At the same time, the Ag additive increases the intragranular connectivity, mechanical strength and superconducting grain size. Thus, it also improves the superconductivity performance [31, 32]. When the polarized optical photographs of the TSMG samples were examined, the presence of different colour distribution regions was not observed. This indicates that the samples do not contain grains with different orientations and grain boundaries. The polarized optical photographs show only a portion of the sample. However, in the optical examination, the sample consisted of a single-grain. This is also already supported by the XRD graphs.

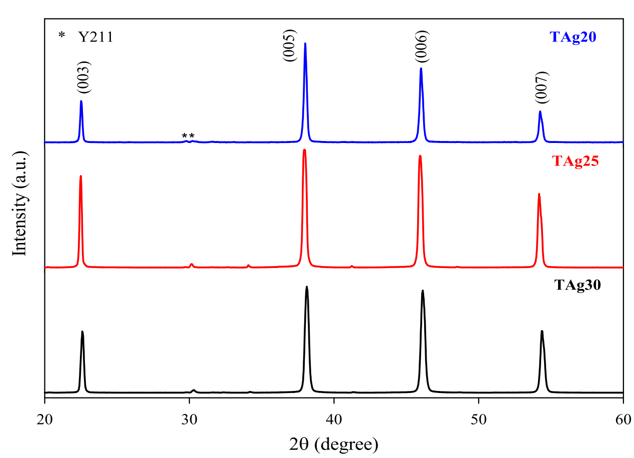

Fig. 3 XRD patterns of TSMG samples

The trapped magnetic field distributions of all Ag-added samples are shown in Fig. 5. The presence of several peaks close to each other was observed in the trapped field profiles of the MAg20, MAg25 and MAg30 samples. These show that the MPMG samples have a granular structure. However, the separation between the peaks is not deep, suggesting that the grain boundaries are clean and the intergranular connectivity is good. The uniformity of the trapped field profile and the height of the peak value indicate the quality of the sample in terms of the properties required for practical applications [33]. If the value of the trapped magnetic field is high, the current carrying capacity of the superconducting materials must be high and the magnetic fluxes must be effectively fixed within the material. Thus, the intensity of the magnetic field trapped by the superconducting

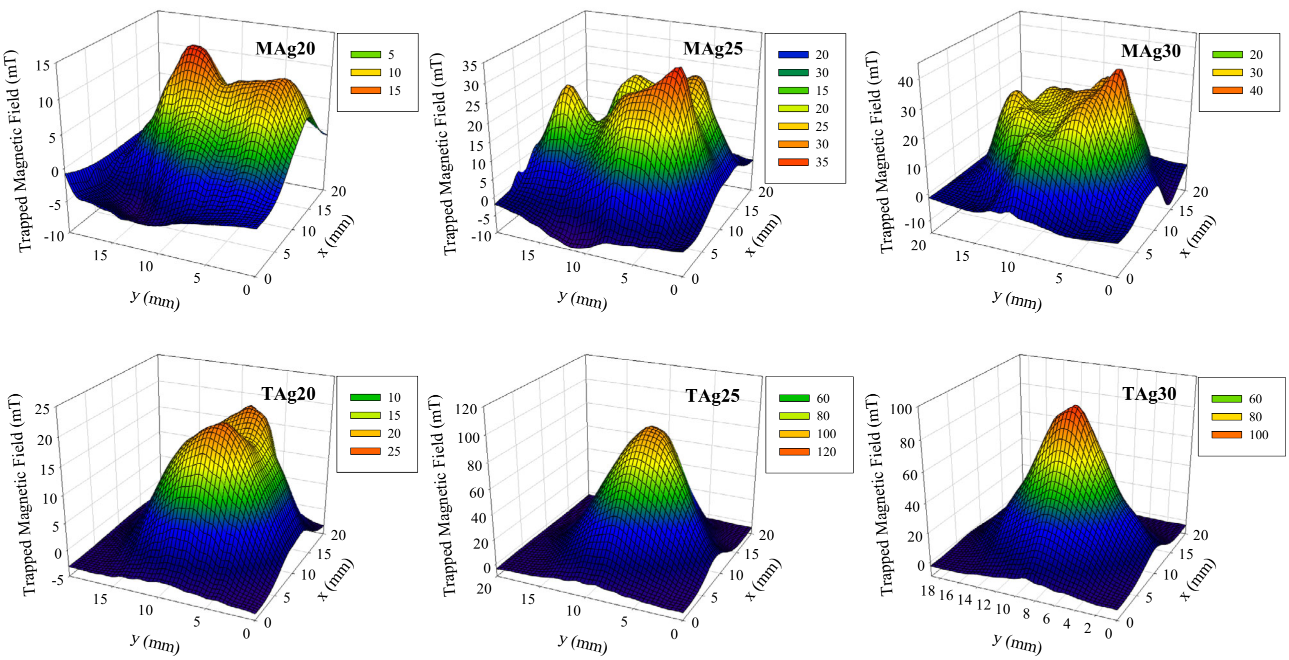

Fig. 5 The trapped magnetic field profiles

samples becomes related to J_c such as $B_{trap} = AJ_c r$, where A is a geometric constant that depends on the shape and aspect ratio of the superconducting sample and r is radius of the sample [34]. It was observed that when the Y211 contribution ratio of the MPMG samples increased, their field trapping abilities also increased. It is known that non-superconducting phases and structural defects (dislocations, grain boundaries, etc.) are used as effective pinning centers in superconducting materials. Larger J_c results in more trapped magnetic field [24]. In this case, the critical current densities of the samples that can trap higher magnetic fields are also expected to be higher. This means that the superconducting properties of the samples are good.

When the trapped magnetic field distributions of TAg20, TAg25 and TAg30 samples were examined, it was observed that although the trapped magnetic field distributions of TAg25 and TAg30 samples was cone-shaped, the single cone shape was distorted and the presence of a small peak that was not discrete from main peak in the trapped magnetic field distribution of TAg20 sample. Due to the fact that these peaks are not very discrete from each other, it is thought that the connectivity between the grains is good, although the single-grain state is deteriorated. The fact that the cone shape is single indicates that the sample is single-crystal [35]. The peaks deeply separate from each other in the trapped magnetic field distributions of the samples produced by the multi-seeded melt growth (MSMG) method. This means that the grain boundaries act as weak couplings, there is no supercurrent along these boundaries and thus reducing the trapped magnetic field value in these regions [33, 36]. At the same time, it was observed that the highest magnetic field value belonged to the TAg25 sample.

High trapped magnetic fields and therefore high critical current densities can be obtained with superconducting bulks produced by TSMG and MPMG methods. The variation of the levitation force values per unit volume, which is known to be related to the critical current density and measured in ZFC regime at 77 K, to vertical displacement is shown in Fig. 6. As the distance between the superconductor and the permanent magnet decreased, the existence of a repulsive force caused by the Meissner effect was observed. In the case of Meissner, the repulsive force is at its maximum value since the applied magnetic field did not penetrate into the sample. Among the MPMG samples, the MAg30 sample has the highest repulsive force value. The maximum value of the

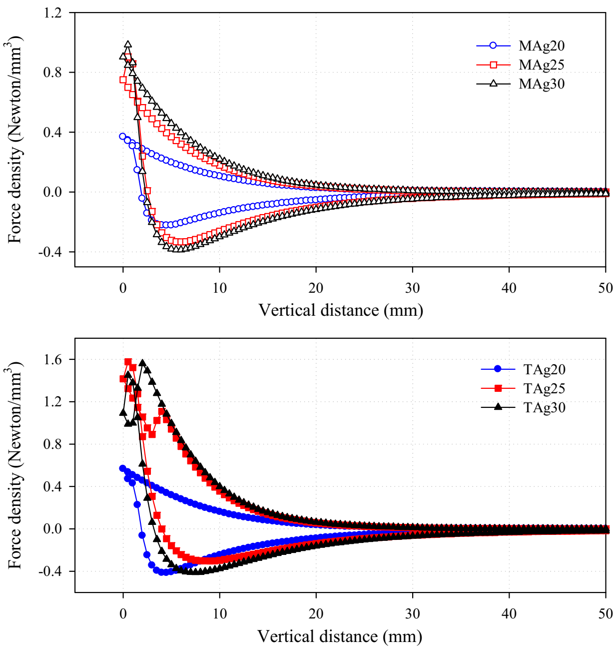

Fig. 6 The vertical levitation force curves in ZFC regime and different cooling distance at 77 K

vertical repulsive force of TAg25 and TAg30 samples is the highest compared to the other samples. In Fig. 5, it is seen that the trapped magnetic field values of TAg25 and TAg30 samples with high repulsive force observed in Fig. 6, are higher than the others. The magnitude of the force between a permanent magnet and a superconductor depends on the quality of the superconducting material and its ability to screen the applied external magnetic field. If the critical magnetic field is the larger, the repulsive force is the higher [37]. Thus, it is expected that trapped magnetic field values of TAg25 and TAg30 samples will be high as well as the critical current densities. At the same time, it is seen that the levitation force density increases with the increase amount of Y211 additive. It is known that non-superconducting Y211 particles act as fluxpinning centers, similar to oxygen vacancies, dislocations and stacking defects in the material [22].

When the permanent magnet is brought closer to the superconductor, the applied external magnetic field and thus the—M magnetization increases. When the magnet is removed from the superconductor, the external magnetic field decreases, but some magnetic field traps inside the superconductor. This gives rise to + M magnetization which causes a reduction in the repulsive force occurs. In this case, the magnitude of the repulsive force decreases. After a certain point, the force changes direction and the attractive force emerges [38]. In many studies, it has been observed that the repulsive and attractive forces that occur when the distance between the YBCO superconductor and the permanent magnet change, exhibit a hysteresis behavior. [22, 39–41]. These hysteresis curves strongly depend on the size of the grains and the intergrains connectivity in the superconductor [42]. The width of the hysteresis curve formed by the repulsive and attractive forces is a measure of the flux-pinning potential of the superconductor. Thus, if hysteresis width is the larger, the flux-pinning potential is the stronger [43]. In Fig. 6, it is seen that the hysteresis widths of the TAg25 and TAg30 superconductor samples are the largest.

4 Conclusion

The results obtained in this study, which was aimed to determine the most suitable production method and the most suitable composition, in order to ensure that the silver-added YBCO samples, which can be used as addition material, have high superconductivity properties, are as follows:

1. MPMG YBCO samples have a dominant superconducting structure and preferential orientation partially in the *c*-axis direction.
2. TSMG YBCO samples are single-crystal samples highly oriented along to the *c*-axis.
3. The trapped magnetic field value of the TAg25 sample is the highest, and at the same time, the maximum values of the repulsive force of the TAg25 and TAg30 samples are the highest.
4. The hysteresis widths of these samples are also higher than the other samples, indicating that their flux-pinning potential is high.

It is important that the solder materials used in the welding of the bulk superconductors must not prevent the flow of supercurrent in the welding region and the solder material must have a lower melting temperature than the main samples. Ag_2O additions lowers the melting temperature of the YBCO sample. Superconducting properties of the YBCO sample can be improved with appropriate additions and production method. In this way, solder material, having basic superconductor parameters close to the main bulks to be welded, can be obtained. In this study, it was observed that the solder material produced in the composition Y123 + 25%Y211 + 20%Ag_2O by the TSMG method exhibited higher superconducting properties than the other samples. Therefore, the sample obtained is a suitable candidate as a solder material.

Acknowledgements

This study was supported by Karadeniz Technical University research grant (FDK-2018-7181, FHD-2021-9349).

Author contributions

All authors contributed to the study conception and design. Material preparation, data collection and analysis were performed by ŞD, BÇ, MB, TK and AA. The first draft of the manuscript was written by ŞD and all authors commented on previous versions of the manuscript. All authors read and approved the final manuscript.

Funding

This study was supported by Karadeniz Technical University research grant (FDK-2018-7181, FHD-2021-9349). The authors declare that no funds, grants, or other support were received during the preparation of this manuscript.

Data availability

All data generated or analysed during this study are included in this published article.

Declarations

Conflict of interest The authors have no conflicts of interest to declare that are relevant to the content of this article.

References

1. T.A. Prikhna, Modern superconductive materials for electrical machines and devices working on the principle of levitation. Fiz. Nizk. Temp. **32**, 661–676 (2006)
2. D.K. Namburi, Y. Shi, D.A. Cardwell, The processing and properties of bulk (RE)BCO high temperature superconductors: current status and future perspectives. Supercond. Sci. Technol. **34**, 053002 (2021)
3. B. Çakır, A. Aydıner, Structural and magnetic properties of the ring shaped 40 wt% Y211 added TSMG Y123 bulk superconductors welded by Ag_2O added MPMG YBCO solder material. J. Mater. Sci. **28**, 17098 (2017)
4. J.V.J. Congreve, Y.H. Shi, A.R. Dennis, J.H. Durrell, D.A. Cardwell, Growth rate of YBCO-Ag superconducting single grains. IOP Conf. Ser. **279**, 012027 (2017)
5. J. Sheng, M. Zhang, Y. Wang, X. Li, J. Patel, W. Yuan, A new ring-shape high-temperature superconducting trapped-field magnet. Supercond. Sci. Technol. **30**, 094002 (2017)
6. L. Chen, H. Claus, A.P. Paulikas, H. Zheng, B.W. Veal, Supercond. Sci. Technol. **15**, 672 (2002)
7. G. Wei, Z. Guisheng, C. Xiao, W. Aiping, H. Jiarun, B. Hailin, R. Jialie, J. Yulei, Joining of textured YBCO with YBCO added Ag_2O additive. Phys. C **470**, 482 (2010)
8. J.V.J. Congreve, A.R. Dennis, Y. Shi, C.W. Bumby, H. Druiff, D.A. Cardwell, J.H. Durrell, A reliable technique to fabricate superconducting joints between single grain, Y–Ba–Cu–O bulk superconductors. Supercond. Sci. Technol. **34**, 094003 (2021)
9. P. Diko, G. Fuchs, G. Krabbes, Influence of silver addition on cracking in melt-grown YBCO. Phys. C **363**, 60 (2001)
10. T. Puig, P. Rodriguez Jr., A.E. Carrillo, X. Obradors, H. Zheng, U. Welp, L. Chen, H. Claus, B.W. Veal, Crabtree, self-seeded YBCO welding induced by Ag additives. Phys. C **363**, 75 (2001)
11. T. Hopfinger, R. Viznichenko, G. Krabbes, G. Fuchs, K. Nenkov, Joining of multi-seeded YBCO melt-textured samples using YBCO/Ag composites as welding material. Phys. C **398**, 95 (2003)
12. A. Altınkök, K. Kılıç, M. Olutaş¸, A. Kılıç, Magnetovoltage measurements and hysteresis effects in polycrystalline superconducting $Y_1Ba_2Cu_3O_{7-x}$/Ag in weak magnetic Fields. J. Supercond. Nov. Magn. **26**, 3085 (2013)
13. P. Rani, R. Jha, V.P.S. Awana, AC susceptibility study of superconducting $YBa_2Cu_3O_7$:Ag_x bulk composites (x = 0.0–0.20): the role of intra and intergranular coupling. J. Supercond. Nov. Magn. **26**, 2347 (2013)
14. T. Metin, M. Tepe, The effect of Ag doping on the superconducting properties of $Y_3Ba_5Cu_{8-x}Ag_xO_{18-\delta}$ ceramics. J. Supercond. Nov. Magn. **30**, 1083 (2017)
15. J.V.J. Congreve, Y. Shi, K.Y. Huang, A.R. Dennis, J.H. Durrell, D.A. Cardwell, Improving mechanical strength of YBCO bulk superconductors by addition of Ag. IEEE Trans. Appl. Supercond. **29**, 6802305 (2019)

16. K. Iida, T. Kono, T. Kaneko, K. Katagiri, N. Sakai, M. Murakami, N. Koshizuka, Joining of different Y–Ba–Cu–O blocks. Phys. C **402**, 119 (2004)
17. A.L.L. Jarvis, M. Pillay, Joining of bulk high temperature superconductors. J. Phys. **43**, 434 (2006)
18. M. Sefcikova, P. Diko, B. Bozzo, X. Granados, X. Obradors, Influence of crystal plane on the welding quality of YBCO bulk superconductor. Mater. Sci. Eng. B **151**, 107 (2008)
19. E. Bartolomé, J.J. Roa, B. Bozzo, M. Segarra, X. Granados, Effective silver-assisted welding of YBCO blocks: mechanical versus electrical properties. Supercond. Sci. Technol. **23**, 045013 (2010)
20. M. Rottaa, D.K. Namburi, Y. Shib, A.L. Pessoac, C.L. Carvalhoc, J.H. Durrell, D.A. Cardwell, R. Zadorosnyc, Synthesis of Y_2BaCuO_5 nano-whiskers by a solution blow spinning technique and their successful introduction into single-grain. Ceram. Int. **45**, 3948 (2019)
21. J.G. Noudem, E.S. Reddy, M. Tarka, M. Noe, G.J. Schmitz, Melt-texture joining of $YBa_2Cu_3O_y$ bulks. Supercond. Sci. Technol. **14**, 363 (2001)
22. B. Çakır, K. Öztürk, S.B. Güner, Å. Çelik, A. Aydıner, Magnetic properties of the welded joined TSMG Y123 + x wt% Y211 (x = 20 and 30) bulk superconductors. Phys. C **557**, 19 (2019)
23. A. Ates¸, E. Yanmaz, The effects of Ag addition and magnetic field on melt-processed $YBa_2Cu_3O_x$ superconductors. J. Alloys Compd. **279**, 220 (1998)
24. M. Başoğlu, The effect of grain growth temperature on the trapped magnetic field of Y358 superconductors. J. Supercond. Nov. Magn. **34**, 117 (2021)
25. B. Çakır, A. Aydıner, Preparation and properties of MPMG YBCO bulk with Y_2O_3 layer. J. Supercond. Nov. Magn. **24**, 1577–1584 (2011)
26. T. Kruaehong, Electrical properties and crystal structure of Y123, Y358 and Y257/Y211 composite bulk superconductors. Int. J. Phys. Sci. **9**(16), 360–367 (2014)
27. M.S.M. Suan, N.A. Hasim, M.E.A. Manaf, M.R. Johan, Effects of Ag_2O nanoparticles addition on electrical conductivity and microhardness properties of polycrystalline $YBa_2Cu_3O_{7-\delta}$. Chin. J. Phys. **55**, 1857–1864 (2017)
28. G.-Z. Li, X.-Y. Deng, L. Dong, Facile fabrication of nanocomposited Y-Ba-Cu-O single-grain superconductor using raw metallic oxides. Mater. Chem. Phys. **167**, 14–17 (2015)
29. T. Chaieb, D. Brouri, S. Casale, J.-M. Krafft, T. da Silva, C. Thomas, L. Delannoy, C. Louis, On the origin of the changes in color of Ag/Al_2O_3 catalysts during storage. Res. Chem. Intermed. **45**, 5877–5905 (2019)
30. B. Çakır, Effect of the heat treatment applied during the welding process on superconducting properties of the welded YBCO samples. IEEE Trans. Appl. Supercond. **33**, 2 (2023)
31. M. Tepe, I. Avci, H. Koçoğlu, D. Abukay, Investigation of the variation in weaklink profile of $YBa_2Cu_{3-x}Ag_xO_7$-δ superconductors by Ag doping concentration. Solid State Commun. **131**, 319 (2004)
32. P. Rani, A. Pal, V.P.S. Awana, High field magneto-transport study of $YBa_2Cu_3O_7$:Ag_x (x = 0.00–0.20). Phys. C **497**, 19 (2014)
33. Y. Shi, A.R. Dennis, D. Zhou, D.K. Namburi, K. Huang, J.H. Durrell, D.A. Cardwell, Cryst. Growth Des. **16**, 5110 (2016)
34. M. Murakami, Measurements of trapped-flux density for bulk high-temperature superconductors. Phys. C **357–360**, 751–754 (2001)
35. S.P.K. Naik, M. Miryala, M.R. Koblischka, A. Koblischka-Veneva, T. Oka, M. Murakami, Production of sharp-edged and surface-damaged Y_2BaCuO_5 by ultrasound: significant improvement of superconducting performance of infiltration growth-processed $YBa_2Cu_3O_{7-\delta}$ bulk superconductors. ACS Omega **5**, 6250 (2020)
36. A. Almalki, D.K. Namburi, M. Ba-Abbad, A.R. Dennis, K.Y. Huang, A. Almutairi, J.H. Durrell, D.A. Cardwell, Processing and properties of bar-shaped single-seeded and multi-seeded YBCO bulk superconductors by a top-seeded melt growth technique. J. Supercond. Nov. Magn. **30**, 1397 (2017)
37. E. Várguez-Villanueva, V. Rodríguez-Zermeño, V. Sosa, Calculation of vertical force between finite, cylindrical magnets and superconductors. Rev. Mex. Fís. **54**, 293 (2008)
38. M. Murakami, T. Qyama, H. Fujimoto, T. Taguchi, S. Gotoh, Y. Shiohara, N. Koshizuka, S. Tanaka, Large levitation force due to flux pinning in YBaCuO superconductors fabricated by melt-powder-melt-growth process. Jpn. J. Appl. Phys. **29**, 1991 (1990)
39. K. Özturk, M. Kabaer, M. Abdioglu, A. Patel, A. Cansiz, Clarification of magnetic levitation force and stability property of multi-seeded YBCO in point of supercurrent coupling effect. J. Alloys Compd. **689**, 1076 (2016)
40. L. Quéval, K. Liu, W. Yang, V.M.R. Zermeño, G. Ma, Superconducting magnetic Bearings simulation using an H-formulation finite element Model. Supercond Sci. Technol. **31**, 084001 (2018)

41. A.N. Maksimova, I.A. Rudnev, V.A. Kashurnikov, A.N. Moroz, Levitation forces acting on an HTS sample in the field of a permanent magnet. J. Supercond. Nov. Magn. **35**, 3093 (2022)
42. Ä. Karaca, A comparative study for magnetic levitation force in type-II superconductors. Sak. Üniv. Fen Bilimleri. Enst. Derg. **21**, 1293 (2017)
43. K. Özturk, S. Çelik, A. Cansiz, Determination of levitation force and pinning properties of $(Sm123)_{1-x}(Yb211)_x$ bulk superconductor depending on Yb211 doping ratio. Phys. Status Solidi A **206**, 2569 (2009)